**MDPI**

*Article*

# A Techno-Economic Analysis of a Cargo Ship Using Flettner Rotors

**Gianluca Angelini \*, Sara Muggiasca \*** and **Marco Belloli \***

Mechanical Engineering Department, Polytechnic University of Milan, Via La Masa 1, 20156 Milan, Italy
* Correspondence: gianluca.angelini@polimi.it (G.A.); sara.muggiasca@polimi.it (S.M.);
  marco.belloli@polimi.it (M.B.)

**Abstract:** In the last twenty years, the global shipping transport demand has strongly increased (around 4% per year since the 1990s), together with the request for new green propulsion technologies to break down carbon emissions and face the costs deriving from the usage of conventional diesel fuels. Flettner rotors (hereafter: FRs) have been identified by several researchers as a promising solution to exploit wind energy on commercial ships, reducing fuel consumption. The present work presents a six-degree-of-freedom (6DOF) ship performance model set up to evaluate the best way of using a pair of Flettner rotors. The study analyses the performance of this propulsion system in consideration of weather and sea conditions, evaluating the related reduction in fuel consumption. A discussion about the economic and environmental advantages of the usage of FRs is provided, considering the costs linked to their installation and the new emission restrictions. Relevant results have been obtained for different routes, speed ranges and rotor dimensions while investigating the best Flettner rotor arrangement to minimise both the emissions and the installation cost payback period.

**Keywords:** Flettner; rotors; ship; fuel saving; Matlab; 6DOF; simulation

---

## 1. Introduction

Shipping alone is estimated to have generated 3% of the total industrial world $CO_2$ emissions in 2018, growing to 4.9% in 2021 [1]. The attention to the environmental implications has proportionally increased, with the pressure on the technology sectors to research new sustainable solutions becoming more and more considerable. In the last 20 years, technical progress and research have received an important booster from the restrictive regulations ratified by the majority of the more industrialised and, therefore, more polluting countries.

The North Atlantic Treatment Organization (hereafter, NATO) has currently promoted several regulations and protocols about the usage of green energy, contributing to lower fuel consumption and, consequently, to lower polluting gas inlets into the air. Among various types of alternative energy, wind has been considered the easiest to become a potential source of energy for ships in the last 20 years.

Different types of wind energy are under analysis in engineering research since interesting results can be obtained using rigid sails or cylindrical rotors, such as highlighted by P. Zhang [2] and N. Ammar [3]. Relevant conclusions have been drawn by A. Schönborn in his studies about the functioning of Darrius rotors [4], by A. Kramer regarding the comparison between wing sails and Flettner rotors [5] and by M. Traut et al. concerning the usage of a kite on selected shipping routes [6]. Indeed, increasing fuel prices are shoving research towards new, alternative solutions to internal combustion engines for maritime transportation; this is why all these wind-assisted systems are being seriously reconsidered. Although the widespread availability of studies about new cleaner alternative fuels [7] or low-sulfur residue marine fuels [8], this paper will focus on the usage of Flettner rotors as wind-assisted propulsion for maritime transportation due to the availability of a large experimental data campaign personally collected in the Politecnico di Milano Wind Tunnel.

In order to investigate how FRs can be optimised for usage on board ships, a computer-based study will be presented in the present work, as well as the deriving economic evaluations and considerations. The aim is the implementation of simulation models written in Matlab and simulating the behaviour of the ship while sailing, with the goal of minimising fuel consumption. To make these calculations as real as possible, the code automatically downloads the weather data from the web for all the simulations. Considering a cargo ship as a case study and four different routes, several six-degree-of-freedom simulations have been conducted to numerically evaluate the benefits coming from the usage of FRs aboard. Mathematically, the code created for the estimation of the fuel reduction can be considered as an alternative to the NAPA Voyage Optimisation software, available on the web for academic studies and commercial use to predict and optimise ship routes and fuel consumption. Indeed, the code discussed in the present work is built up to evaluate simultaneously the intact stability and manoeuvrability criteria, hence the comparison with the following specific tool provided by NAPA: the NAPA Stability software. As a matter of fact, the present work differs from the one conducted by R. Lu et al. because of their choice of a four-degree-of-freedom ship model [9], but even in this case, the results are comparable. In the end, the most important parameters influencing the costs of the installation of FRs aboard are discussed in the last paragraph in order to evaluate their economic impact on the payback period of Flettner rotors.

## 2. The Importance of Simulations

Every industrial process, even when starting with not so clear and easily predictable results, has guaranteed better results or predicted worse results if subjected to a computer management process. As explained by D. Sandaruwan in his paper [10], a six-degree-of-freedom simulation of ship motions allows the evaluation of different scenarios and how the ship responds to external phenomena. Indeed, the implementation and operational cost of a computer simulation system is only a fraction of the conventional trials involving models and real ships. Especially in the naval field, where costs related to new model-based experimental campaigns are often huge, the ability to perform simulations regarding the behaviour of a ship when exposed to specific or generic external conditions represents a very profitable advantage for the shipowner in terms of money and time. Other similar works aiming to predict and simulate the ship motions in general external conditions are provided by G. Taimuri [11] and G. Barauskis [12].

In the work presented in this paper, the benefits of the installation of FRs aboard a cargo ship will be investigated through a code written to create a power prediction program. By using computer technology offered by commercially available softwares—specifically Matlab R2018b® and Maritime DelftShip v11.10®—the code has been conceived to evaluate a ship operating on commercial trades while optimising the usage of this new system in order to meet the requirements of annex VI of MARPOL. Thanks to Matlab®, the equilibrium equations of the forces acting on the ship are solved in an iterative way, aiming to find the best compromise between rotors' contribution to forward speed and stability criteria. Equally, the Maritime DelftShip® software has been essential to obtain the main physical and geometrical properties of the cargo ship considered as a case study, such as the inertial characteristics and the 3D position of the centre of buoyancy and gravity.

As no investment from an environmental perspective can be made without consideration of its financial implications, the code ends with an economic estimation of the saved money. Thanks to the provided optimisation of the route, the better and more widespread the usage of rotors, the cheaper the shipping.

## 3. The Structure of the Code

The code is made of sub-routines, each one responsible for the solution of a specific part of the FRs usage-related optimisation problem during navigation. While the geographic setting of the problem is solved with the generation of a matrix necessary to cover the track by sea, the physics and mathematics formulae describing the ship motions have

been divided into different sub-functions due to the complexity of the 6DOF problem and the necessity to linearise the calculation of manoeuvrability and stability second-order parameters. All six motions are assumed to vary slowly and step-by-step and are represented by the linear relations of forces and motion components. Indeed, the effects of shallow water are assumed to be negligible.

Similar models are available in the literature [13], realised to combine the ship manoeuvrability with the latest Energetic Efficiency Design Index (EEDI) requirements by the International Maritime Organization (IMO) regulations. Like Sprenger in his work, the hydrodynamic components of the still water resistance and manoeuvering derivatives in calm waters have been considered in the present study, together with the effects of vessel drift and rudder angle when added resistance in waves is accounted for, as suggested by Tillig and Ringsberg in their work [14].

Several parameters, such as properties derived from the Maritime DelftShip® calculation or the velocity range, are variable to users' liking in order to keep the code completely customisable.

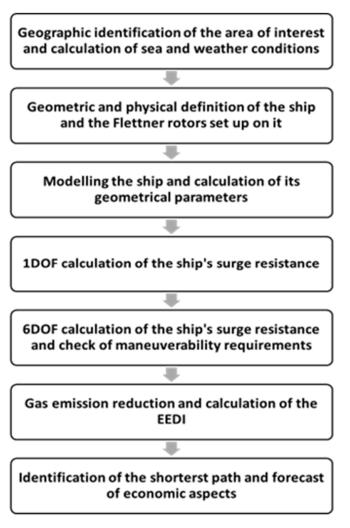Figure 1 represents a flow chart highlighting the main steps performed by the code as follows:



**Figure 1.** Code flow chart.

*3.1. The Map*

When the code starts, users are required to identify a departure and an arrival point on a planisphere pop-up, as shown in Figure 2.
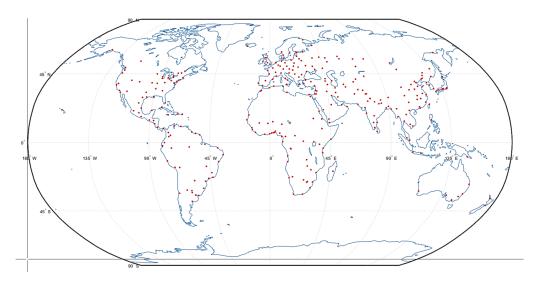
**Figure 2.** Choosing the departure and arrival points on the map.

When both the parameters latitude (LAT) and longitude (LONG) have been identified for the chosen points, the program elaborates a $400*200$ matrix, which identifies all possible LAT-LONG combinations for the ship position on the map during its transfer (an example of this matrix is provided in Figure 3).
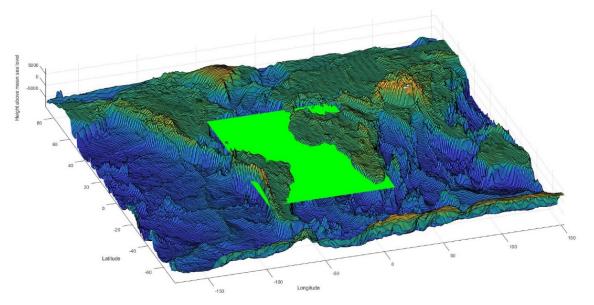


**Figure 3.** Example of navigable points of the route matrix.

The points belonging to the above-mentioned matrix represent—at this stage of the code—the totality of the possible geographical points for the case study. In fact, every element of the matrix represents the potential geographical position the ship is eligible to take on. Furthermore, the same importance needs to be accredited to the links among the aforementioned elements due to the physical sense they hold. In fact, every matrix element offers a vectorial link with the eight surrounding elements. These eight links, shown in Figure 4, represent eight possible steps for the creation of the best path; this is why the code has been structured to compute the resistance of the 6DOF ship model for every single step in order to calculate the final shortest path.
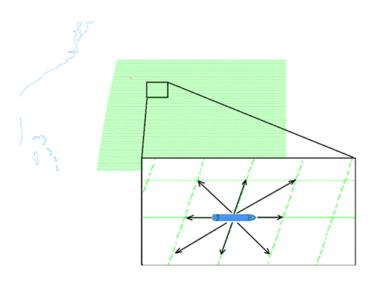
**Figure 4.** Overview on the matrix elements.

When the matrix has been geographically set, the second step of the code regards the identification of the weather environment. At this stage, users define a specific day of the year, which the performance prediction program (hereafter, PPP) uses to extrapolate the intensity and the direction of the absolute wind on a global scale from the US National Oceanic and Atmospheric Administration (NOAA) database available online in GRIB2 format files on https://nomads.ncep.noaa.gov (accessed on 4 July 2022).

$$\text{Data Input} = [W_{module}; W_{direction}] \tag{1}$$

where:

- $W_{module}$ is the wind absolute intensity;
- $W_{direction}$ is the wind direction in global reference system.

This operation is computed every time users want to upload the weather data taken into account by the code. The authors have chosen the US database, but other sources on the web can offer the same data on a global scale, such as the weather routing software supplied by NAPA, a Finnish maritime software, service and data analysis provider. Once these data have been downloaded, the code arranges them in order to match every single point of the above-mentioned matrix with a specific and real weather conditions and completes all the simulation steps by considering the weather always the same. In this study, the weather conditions of 4 July 2022 have been taken into account, but if users want to have an updated calculation of the best route in order to consider more updated weather data, a new execution of the code is always possible.

During simulations, the ship's speed and environmental conditions are assumed to be constant for the whole navigation. Indeed, a maximum engine speed is always considered a superior limit of functioning. While sailing with particular adverse weather conditions, if the engine break power exceeds this limit, the code equals the engine speed to this value. This possibly results in later arrival times.

### 3.2. The Rotors

A fluid—in this case, air – striking a body tends to meet resistance when it impacts the body and, due to the principle of continuity, it makes its previously separated fluid fillets closer behind the body, creating whirling phenomena and turbulence.

The first researchers able to predict the potentiality of this physical phenomenon were the German engineers Flettner and Savonious in 1925 [15]. Over the past years, Flettner was able to use rotating cylinders as a valid alternative to fuel for ship propulsion [16]. Flettner's results were mathematically confirmed by Prandtl's studies on the Magnus effect [17]. In fact, he theorised that if a cylindrical body, rather than stationary, is put into rotation, it

tends to facilitate the passage of the fluid fillets in harmony with its direction of rotation, generating a decrease in the flow density and consequently in pressure with respect to the opposite side. This difference in pressure between the two sides of the body produces, physically, a shift from the equilibrium position towards the overpressure field, as shown in Figure 5.
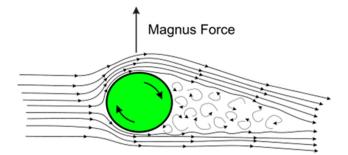


**Figure 5.** Fluid interaction with a rotor.

Consequently, the effect generated is aerodynamically comparable to the one generated by an airfoil hit by a fluid, which develops resistance parallel to the direction of the fluid and lifts it transversely. Furthermore, in his studies [18] in collaboration with A. Thom, Flettner analysed the influence of several parameters on the behaviour of rotating cylinders— i.e., endplates, Reynolds number (Re), speed ratio (SR) and aspect ratio (AR)—pointing out that an endplate reduced the losses of fluid and, consequently, the lift decline of the rotating cylinder as follows [18]: he demonstrated that the best effect was achievable with the use of an endplate having 1.5 times the diameter of the cylinder. In fact, several recent studies conducted by T.J. Craft [19], A. De Marco [20] and W. Zhang [21] have confirmed Flettner's claims.

For the cargo ship used in the research as a case study, it was decided to simulate two rotors installed in a longitudinal configuration and with a mutual 15D distance, according to the schematic representation provided in Figure 6 and Table 1 as follows:
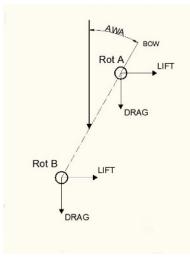


**Figure 6.** Arrangement of the rotors.

**Table 1.** Rotors working parameters.

| Formula | Description |
|---|---|
| Max thrust = 100 kN | Maximum payable value of thrust |
| $X_{aft}$ = 40 m | Longitudinal position of the aft rotor from aft |
| $X_{forward}$ = 85 m | Longitudinal position of the forward rotor from aft |

With the Flettner rotors on the diametral plane of the ship, no other measures are required to increase the manoeuvring capabilities; no larger or more effective rudders are needed; additional appendages do not have to be considered. The mass of every rotor has been calculated considering each one of them as empty cylinders—with a thickness of 1.3 m—and made of carbon-fibre-reinforced polymers (CFRP, having density = 0.6 g/cm³).

A specific sub-function of the code has been developed to calculate the apparent wind direction (the β angle of Figure 7) with respect to the ship bow based on the ship direction and the real wind direction and module. A similar approach is suggested by De Marco in his work [20].
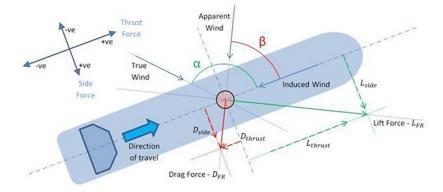


**Figure 7.** Representation of the forces acting on a rotor, reproduced from [22], with permission from David Pearson, 2022.

The coefficients $C_{Lift}$ and $C_{Drag}$ necessary for the evaluation of lift and drag generated by the rotors have been calculated through experimental tests in the wind tunnel at POLIMI. Appropriate comments are provided by Bordogna in his work [23].
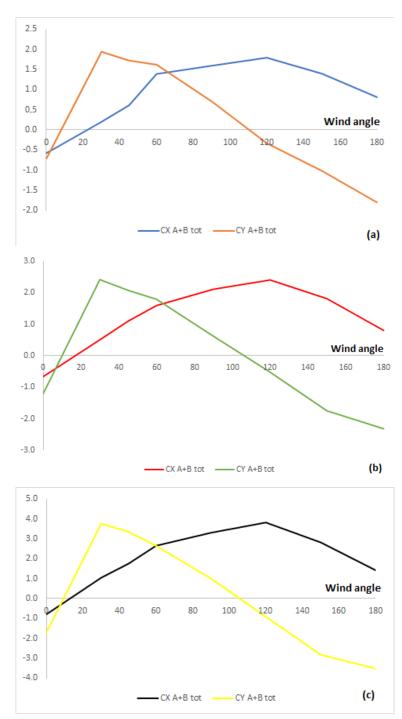
For reference, the above tests were carried out by measuring $C_{Lift}$, $C_{Drag}$ and $C_M$ in an experimental data campaign with two rotors acting at different mutual distances. Figure 8 shows a configuration where rotors had a distance between their axes of rotation equal to fifteen times their diameter (15D), but 3D and 7.5D arrangements have also been investigated during wind tunnel tests. A flow with an altered value of SR among 1, 1.5, and 2, respectively, have been examined, maintaining the value of the blowing wind equal to $Re = 1.0 \times 10^5$.



**Figure 8.** Rotors in a 15D distance configuration during the wind tunnel.

Values of the longitudinal coefficient $C_x$ and of the transversal coefficient $C_y$ have been obtained by summing up the projections of lift and drag coefficients $C_{Lift}$ and $C_{Drag}$ along the longitudinal and transverse axes, as explicated in the following formula:

$$C_x = C_{Drag\ long} \cdot \sin(\beta) + C_{Lift\ long} \cdot \cos(\beta) \tag{2}$$

$$C_y = C_{Drag\ transv} \cdot \sin(\beta) + C_{Lift\ transv} \cdot \cos(\beta) \tag{3}$$

The achieved results are shown in Figure 9:



**Figure 9.** $C_X$ and $C_Y$ calculated from wind tunnel tests in a 15D arrangement for: (**a**) SR = 1 for both rotors; (**b**) SR = 1.5 for both rotors; (**c**) SR = 2 for both rotors.

Subsequently, the PPP calculates the longitudinal and transverse forces generated by rotors and acting on the ship using the following formulae:

$$F_x = \frac{1}{2} \cdot C_X \cdot \rho_{air} \cdot D_{cyl} \cdot L_{cyl} \cdot V_{Wind\ app}{}^2 \tag{4}$$

$$F_y = \frac{1}{2} \cdot C_Y \cdot \rho_{air} \cdot D_{cyl} \cdot L_{cyl} \cdot V_{Wind\ app}{}^2 \tag{5}$$

where:

- $\rho_{air}$ is the air density;
- $D_{cyl}$ is the rotor diameter;
- $L_{cyl}$ is the rotor span;
- $V_{Wind\ app}$ is the apparent wind velocity in the local reference system.

In these equations, it is assumed that the rotors operate in an undisturbed airflow. In practice, the incoming airflow can be disturbed when the rotors are placed in proximity of the cargo on deck, superstructures and other rotors. These effects are not taken into account in this study. To prevent significant errors in the rotor force calculations, rotors should be placed at a sufficient distance from objects obstructing the incoming airflow.

### 3.3. The Ship

Considering the trials and measures made by the German society ENERCON GmbH about the E-Ship1 using a four-rotor configuration [24], the choice of a cargo ship with main dimensions comparable to E-Ship1's ones has been followed in this study, having the main dimensions reported in Table 2.

**Table 2.** Main dimension of the Ro-Ro ship.

| Properties | Description |
|---|---|
| $L_{pp}$ = 135 m | Design length between perpendiculars |
| B = 22.5 m | Design beam |
| D = 7 m | Design draft |
| $X_{MS}$ = 65 m | Midship location |
| $C_P$ = 0.6053 | Prismatic coefficient |
| $C_B$ = 0.583 | Block coefficient |

The volume and waterplane properties, such as the lateral plane main dimensions, required by the code to geometrically identify the problem and to solve it, have been extracted through the usage of the free-source external software DelftShip Maritime Software.

Finally, the hypothesis of the installation of two CAT endothermic engines—model MAK VM32-C16—has been chosen for the present case study. They have been considered as fitted on two different shaft lines with $\eta_{shaft}$ equals to 0.98 and by two respective gearboxes, having the following:

$$Ratio_{reduction} = rpm_{shaft}/rpm_{engine} = 1/5 \tag{6}$$

where:

- $rpm_{shaft}$ is the shaft rotation speed per minute;
- $rpm_{engine}$ is the engine rotation speed per minute.

### 3.4. The Resistance Calculation

In analysing the free motion of a ship in the open sea, it is important to evaluate all the types of forces acting on it in a general case. While the hypothesis of small variances from the equilibrium position is still valid, according to which all the components are mutually independent, the code computes the following expression for each ship velocity step and for each vector of the matrix shown in Figure 4.

$$R_{tot\ x} = R_{AW} + R_{ModShip} + R_{Bow} + R_{Friction} \cdot (1 + k_{factor}) + R_{wind\_X} + R_{app} + R_{wave} + R_{rough\_hull} + \sum F_{Rot} \tag{7}$$

where:

- $R_{rough\_hull}$ is the hull rough resistance;

- $R_{rough\_hull}$ is the friction resistance in calm seawater, calculated on the basis of the analogy with the flat sheet, regulated by the ITTC' 57;
- The form factor resistance is a damping force calculated as the product between $R_{Friction}$ and a $k_{factor}$, estimated by following the formulas of Holtrop and Mennen in their studies [25,26];
- $R_{app}$ is the appendages resistance, whose expressions for shafts, rudders and skeg are suggested by DNV;
- $R_{wave}$ takes into account the wave-making and the wave-breaking resistance, calculated with the approximated formulas suggested by Holtrop and Mennen in their work [25], which consider the draught, the beam and the diffraction of waves on the bulbous bow;
- $R_{bow}$ is the additional resistance due to the presence of a bulbous bow, estimated by using approximated formulas [25];
- $R_{ModShip}$ represents the model-ship correlation resistance, which considers the wetted surface of the ship;
- $R_{AW}$ is the added wave resistance obtained through the energetic equivalence between waves, as mathematically explained by Liu et al. in their work [27];
- $R_{Wind\_X}$ is the air resistance acting on the ship structure above sea level and calculated with Isherwood's regression formula;
- $\sum F_{Rot}$ represents the contribution to thrust offered by the Flettner rotors.

To validate the effectiveness of Equation (7), a trial has been conducted by using the Matlab code depicted in the present paper to evaluate the fuel consumption deriving from the ship resistance for the case study described by R.J. Berendschot in his work [28].

Differences between the case study considered in the present paper and the one chosen by Berendschot are related to stricter main dimensions of the ship, the presence of only one rotor, as well as the route, as follows: in fact, in his work, he has considered a wider time range and only the Rotterdam–Casablanca round-trip route. Despite these characteristics, Equation (7) has shown a good match to the result presented by Berendschot differences of 7% and 4% on the Rotterdam–Casablanca travel with and without FR, respectively, and a difference of 3% and 5% on the return route with and without FR, respectively, have been obtained.

### 3.5. A 6-DOF Analysis

In order to make assessments on the ship's stability and manoeuvrability while sailing, the developed PPP performs a dimensionless analysis of the equations of motion also considering a second-order linearised mutual influence among the parameters speed, acceleration and rudder angle $\delta_{Rud}$. This part of the study has been conducted following the nondimensional theory of derivatives proposed by Nomoto [29] and developed by G. Tamiuri [11], which gave particular importance to the interaction between sway and yaw motions. Therefore, the approximate formulas proposed by Clarke et al. [30] have been used since a deterministic mathematical law describing the shapes of the hull and its waterlines is not available.

Indeed, to perform an as close to reality as possible analysis, the code considers a six-degree-of-freedom behaviour for the ship and contemporarily verifies if all displacements and rotations satisfy the limits imposed by regulations.

To do this, small gradual variations from the initial position are iteratively assumed for each of the degrees of freedom listed above and the intensity of each opposing force and righting moment generated by the ship in every DOF have been calculated by applying appropriate conversions through the following rotation matrix in an Eulerian reference system pointed in the ship's centre of gravity (CoG).

$$T_{RollPitchYaw}(\varphi,\psi,\chi) = T_Z(\chi) \cdot T_Y(\psi) \cdot T_X(\varphi) = [(c_\chi \cdot c_\psi, c_\chi \cdot s_\psi \cdot s_\varphi - s_\chi \cdot c_\varphi, c_\chi \cdot s_\psi \cdot c_\varphi + s_\chi \cdot s_\varphi);$$
$$(s_\chi \cdot c_\psi, s_\chi \cdot s_\psi \cdot s_\varphi + c_\chi \cdot c_\varphi, s_\chi \cdot s_\psi \cdot c_\varphi - c_\chi \cdot s_\varphi); \quad (8)$$
$$(-s_\psi, c_\psi \cdot s_\varphi, c_\psi \cdot c_\varphi)]$$

where:

- $T_Z(\chi)$ is the yaw rotation matrix;
- $T_Y(\psi)$ is the pitch rotation matrix;
- $T_X(\varphi)$ is the roll rotation matrix;
- c represents the cosine function;
- s stays for the sine function;
- $\chi$ is the yaw motion;
- $\psi$ is the pitch motion;
- $\varphi$ is the roll motion.

As regards the roll and the pitch, the heeling moments given by the rotors, by the wind impacting the ship structure above the waterline and by the rudders, were calculated, considering the maximum values of $\varphi < 10°$ and $\psi < 15°$.

The previous effects given by the pitching and rolling motions must be added to the pure motion of the yaw $\chi < 15°$. Furthermore, in addition to external forces such as air resistance and forces generated by the rotors, the contribution provided by the sway motion discussed and calculated during the study of the ship manoeuvrability was taken into account for the calculation of the maximum yaw motion.

Indeed, as a consequence of the simultaneous presence of a non-zero inclination, both in the roll and in the yaw, the vertical components of rotors and wind forces represent the main contribution to the heave motion due both to the oblique functioning of the rotors and to the heeling action of the wind, together with the hydrodynamic effect offered by the rudder.

For this motion, a maximum value of $\varepsilon < 2$ m has been considered, while a limit of $\varsigma < 20$ m has been chosen for the sway. This degree of freedom represents the core of the manoeuvrability study conducted by using the aforementioned nondimensional analysis. Indeed, for the sway motion only, the equilibrium interferences generated by the rolling and pitching have been neglected, given the irrelevance of the relative contributions.

### 3.6. Fuel Consumption

Once the mathematical problem relating to the forces and moments generated on a cargo ship that uses FRs has been solved, whether it has been considered in a 6DOF case or, in a more expeditious manner, in a 1DOF case, the technical analysis must necessarily embrace the environmental implications deriving from the use of these alternative systems.

Currently, NATO has promoted several regulations and protocols (Vienna, Montreal, Kyoto), becoming more and more restrictive over the last 50 years to protect the environment by reducing the emissions of the following greenhouse gases:

- Carbon dioxide ($CO_2$);
- Methane ($CH_4$);
- Nitrous oxide ($N_2O$);
- Hydrofluorocarbons (HFC);
- Perfluorocarbons (PFC);
- Sulfur hexafluoro ($SF_6$).

In 2005, 161 IMO member countries signed the MARPOL agreements (the green onesshown in Figure 10).

**Figure 10.** Countries having signed MARPOL agreements.

At this stage, the code incorporates the technical data of the specific fuel consumption SFC of the MAK VM32-C16 installed engines and of the specific production of $NO_X$ supplied by the manufacturer following factory tests shown in Table 3:

**Table 3.** MAK VM32-C16 emissions parameters.

| Properties | Description |
|---|---|
| SFC = 179 ÷ 195 g/kWh | Specific fuel oil consumption |
| $NO_X$ = 1.6 g/kWh | Specific $NO_X$ emissions |

With regard to nitrogen oxide ($NO_X$), the MARPOL Annex VI provides for increasingly stringent rules.

To allow users to simulate any maritime transport route and the case study cargo-ship to be able to navigate in any sea, the engine type considered in our PPP falls into the Tier III category (1.6 g/kWh released against 2.3 g/kWh) required as max limit).

In order to optimise emissions, therefore, the PPP performs the following calculations for each element of the vectors of the route matrix:

- For each value of the required speed range, it calculates the power necessary to move the ship forward and computes the ratio between the portion of power guaranteed by the rotors while contemporary working with the engines and the power considering only endothermic engines working;
- It locates the highest value of this ratio identifying the speed at which, while respecting the manoeuvrability and stability criteria, the functioning of the rotors is optimal in relation to weather and sea conditions encountered by the ship.

$$Best\ working\ conditions\ =\ \max \begin{pmatrix} \dfrac{P_{Engines} \quad (V_{th} = 1^{st}\ step)}{P_{Engines+Rotors} \quad (V_{th} = 1^{st}\ step)} \\ \vdots \\ \vdots \\ \dfrac{P_{Engines} \quad (V_{th} = i^{th}\ step)}{P_{Engines+Rotors} \quad (V_{th} = i^{th}\ step)} \\ \vdots \\ \vdots \\ \dfrac{P_{Engines} \quad (V_{th} = n^{th}\ step)}{P_{Engines+Rotors} \quad (V_{th} = n^{th}\ step)} \end{pmatrix} \quad (9)$$

where:

- $P_{Engines}$ is the brake power required by the ship using only the diesel engines;

- $P_{Engines+Rotors}$ is the brake power considering the use of FRs;
- $V_{th}$ is the i-th velocity of the range;
- $n$ is the number of elements in the speed range.

This method has been chosen by the author to emphasise the focus on the local optimisation of the functioning of the rotors. Once the best ship speed has been found for each element of the vectors of the route matrix, a Dijkstra's algorithm [31] is applied to evaluate the best succession of the single steps analysed, with the aim to bring the ship from the departure to the arrival point chosen. A similar approach has been used by P. Silveira et al. in their work [32] to identify a potential safe route for ships, by using the information contained in the messages broadcasted by ships and recorded by the coastal traffic service centres.

## 4. Economic Aspects

Regardless of the route covered by a ship, every day of stop in port represents a double economic disadvantage for the shipowner as follows: on one hand, the costs for the usage of the quay increase—proportionally to about 15 k€/day as theorised by G. Musolino et al. in their paper [33]—and, on the other hand, the periods of availability for the transport of material at sea, representing the main source of income of the shipping company, decrease. Furthermore, even during navigation, if the cargo ship takes more days than what expected, according to the contract with the client, there are penalties for the delay in delivery.

Therefore, the technical and economic importance of the elaborated code is evident. In addition to reducing the environmental impact, the installation of FRs and the use of this calculation code optimise commercial routes, endorsing the usage of propulsion systems alternative to diesel.

While always taking into account the stability and manoeuvrability criteria—which cannot be disregarded to ensure the safety of the navigation—it is clear that minimising the travel time of a section implies an increase in the mean value of ship velocity and, consequently, an increase in the fuel consumption and in the costs associated with the transfer of the ship. At this point, the code calculates how much diesel has been consumed and, accordingly, how much it has been spent ($) to cover the route during the simulation.

Furthermore, the cost of the heavy fuel oil (HFO) used for engines varies, and the trends of the global raw materials market influence its value. Because of this, and in order to provide users with likely updated data, the code automatically searches on the page https://shipandbunker.com/prices (accessed on 4 July 2022) for the values that the raw materials are traded at on the American stocks and downloads them.

In Figure 11, the trends of the HFO market value are presented to highlight fuel savings relevance because of the increase in its price.
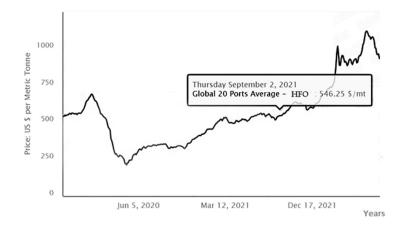


**Figure 11.** HFO price trend from January 2020 to July 2022.

Among the various parameters available to define the cost of fuel, the Global 20 Ports Average was used, which represents the average price of the 20 largest bunkering ports worldwide.

At this point, the code calculates how much diesel has been consumed and, consequently, how many millions of dollars have been spent to cover the route during the simulation. In addition to this, it also provides an estimate of how much money would be saved by using Flettner rotors to their full capacity.

It should be noted that the percentage of $NO_X$ indicated by the code is proportional to the percentage of $CO_2$ omitted from the environment since both parameters have been considered constant as the load of the engines varies. Moreover, from a technical point of view, this percentage value can also be considered a performance parameter as follows: it represents, in fact, how much the propulsive capacity of the ship has been improved.

Without a doubt, the optimisation of the use of Flettner rotors to reduce the emissions of $CO_2$, $NO_X$ e $SO_X$ gives significant results in terms of environmental awareness, but it also represents a substantial and stimulating goal from an economic point of view. In fact, the decrease in the fuel consumption certainly represents an advantageous immediate economic return and is directly proportional to the time of use of the Flettner rotors; yet the improvement of the economic profile is not limited to the sole use of new sources of energy alternative to coal. As a matter of fact, the Norwegian government is proposing new specific taxes proportional to the tons of $CO_2$ emitted into the atmosphere by ships sailing in her waters [34].

In fact, in order to control the emissions of polluting gases in its territory, in 2005, the European Union created the emission trading system (EU ETS) [35]. By making this system mandatory in 2013 and progressively reducing the maximum number of certificates in circulation—which is equivalent to reducing the total amount allowed emissions of polluting gases on an annual basis—the EU has achieved important milestones reaching the $CO_2$ emissions reductions expected by 2030 already in 2020 [36]. On the other hand, the unit price of the certificates has also increased, going from \$8 in 2018 to \$32 in 2020, while it currently stands at around \$90 [37].

*The Formula*

It may be useful, at this point, to summarise the various economic parameters discussed in the following general formula with the aim to create an investment plan for shipowners who want to evaluate the installation of rotors on board their fleet:

$$
\begin{aligned}
\text{rotors}_{\text{benefits}} = &-\text{rotor}_{\text{cost}} \cdot \text{n}_{\text{rotors}} - \text{drydock}_{\text{costs}} - \text{rotor}_{\text{maintenance}} \cdot \text{n}_{\text{rotors}} - \text{refitting}_{\text{time}} - \\
&\text{rotor}_{\text{working}} \cdot \text{n}_{\text{rotors}} + \text{fuel}_{\text{saved}} + \text{fuel}_{\text{cost}} + \text{emission}_{\text{certificates}} + \text{carbon}_{\text{taxes}} + \text{engine}_{\text{maintenance}}
\end{aligned}
\tag{10}
$$

where:

- $N_{\text{ROTORS}}$ is the number of rotors installed aboard;
- $ROTOR_{\text{COST}}$ is the cost of the purchase of each rotor;
- $DRYDOCK_{\text{COSTS}}$ represents all the costs related to the quay stop;
- $ROTOR_{\text{MAINTENANCE}}$ is the parameter describing the rotor periodic maintenance;
- $FUEL_{\text{COST}}$ is the cost of the fuel at the moment of the usage of the code;
- $FUEL_{\text{SAVED}}$ is the amount of fuel saved thanks to the use of the Flettner rotors;
- $ROTOR_{\text{WORKING}}$ is the electrical power absorbed by the rotor;
- $REFITTING_{\text{TIME}}$ is the cost related to the days of stop in shipping;
- $EMISSION_{\text{CERTIFICATES}}$ represents the cost of emitted polluting gases at a company's disposal on an annual and limited-edition basis;
- $CARBON_{\text{TAXES}}$ represents the cost of the amount of $CO_2$ emitted in the air;
- $ENGINE_{\text{MAINTENANCE}}$ represents the cost of the maintenance plans associated with the engines.

In Formula (10), the negative parameters show the costs related to the installation of the rotors and the energy they absorb to rotate, while the positive ones show all savings the rotors generate while working.

The cost for the acquisition of the towers is fixed, and the goal of the shipowner, who embraces this type of alternative propulsion, is to recover the investment over time.

A discussion about the parameters enlisted in the previous expression is provided here below.

- The rotor functioning has a double effect in terms of fuel saving as follows: firstly, the number of tonnes of consumed fuel is proportionally lower while using rotors than with engine propulsion only; secondly, constant growth in fuel price emphasises the benefits deriving from the use of an alternative energy source. In fact, a projection of the fuel price trend was made, analysing the variation in the average cost of fuel over the years. In particular, it was calculated with a regression formula derived from the average value of the Brent fuel fluctuations over the last 10 years downloaded from the web page https://tradingeconomics.com (accessed on 4th July 2022) and presented in Figure 12. The red line tends to represent the average value of the fuel price fluctuation over the years.



**Figure 12.** Crude oil Brent price from 1997 to 2022.

The formula below has been considered to hypothesise the future fuel price following the red line trend:

$$y = (0.75 \cdot x + 35) \cdot z \tag{11}$$

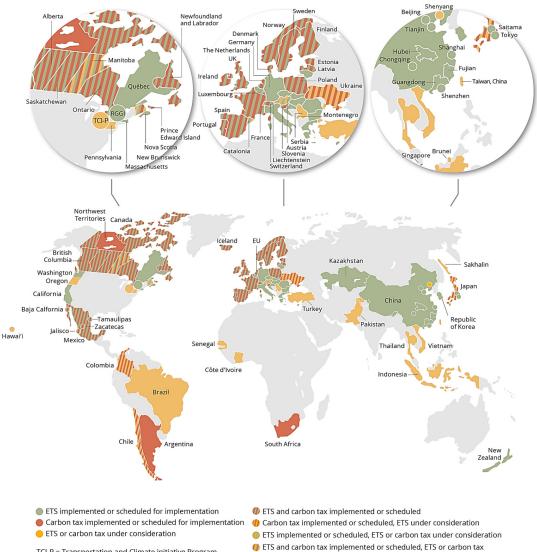where x represents months, y is 1k $, and z are the tonnes of produced $CO_2$.

- A relevant aspect is characterised by the increasing costs shipowners have to bear for carbon emission restrictions and taxes, which have been ratified by every nation in recent years, as explained in the previous paragraphs and shown in Figure 13.

In fact, both emission certificates and carbon taxes have been considered in this paper through the creation of mathematical models simulating the growth in their value from 2012, which the code also contemplates calculating the earnings deriving from the usage of FRs

With regards to the emission taxes, the created mathematical model follows a more than linear and almost parabolic trend, which has grown over the last 5 years with a rather steep trend. This parameter—presented with the red line in Figure 14 and related to the data downloaded from the web page https://tradingeconomics.com (accessed on 4 July 2022)—has been approximated with the following expression:

$$y = [\, 0.05 \cdot (x \cdot 12)^{1.5} \,] \cdot z/1000 \tag{12}$$

where x represents months, y is 1k $, and z are the tonnes of produced $CO_2$.

**Figure 13.** "Global depiction of rules and taxes implemented at July 2022", reproduced from [36].
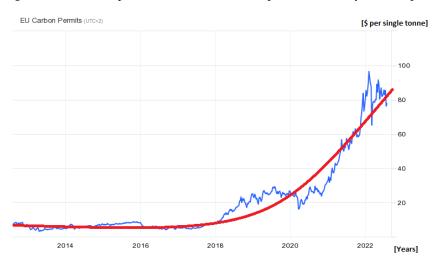


**Figure 14.** $CO_2$ emissions permits price in last decade.

The savings on the due carbon taxes, instead, have been considered as expected to be similar to a mathematical law that is more than linear and can be resumed as follows:

$$y = [\, 0.1 \cdot (x \cdot 12)^{1.2} \,] \cdot z/1000 \qquad (13)$$

where x represents months, y is 1k \$, and z are the tonnes of produced $CO_2$.

- For the purchase of each rotor with dimensions similar to those considered for the cargo ship used as a case study, about $400 \div 500$k \$ costs, including assembly outlays, have been considered. As a matter of fact, further models that can be folded down or equipped with flaps to help reduce vortex phenomena are being more and more preferred [19,38]; therefore, a cost of 500 k\$ is consistent for the acquisition of each rotor. Indeed, for the installation of the rotors, it is necessary to carry out invasive mechanical work both on the hull and on the electrical system on board, given the need to create adequate structural reinforcements on the cross-section to soften the dynamic effects of their operative behaviour in the open sea and bad weather, and the need to electronically configure their operation in couple with the main diesel engines already installed on board. These processes require a stop for the ship and can only be carried out in the drydock.

- Following Apostolidis's works [39,40], the hypotheses enlisted in Table 4 have been made. In addition, a stop in the dock lasting about 20 days with teams working 24/7 for their installation on board, making use of rotors positioned on prebuilt bases by the manufacturer, has been considered as follows:

**Table 4.** Drydock cost for the installation of the rotors.

| Costs [k\$] | Description |
| --- | --- |
| 10.00 | Keel Blocks Plan |
| 9.35 | Drydock Entrance |
| 9.35 | Drydock Exit |
| 7.15 | Drydock occupation |
| 0.50 | Water pumps |
| 0.20 | Lights and electricity |

For the installation work, a total drydock cost of 190 k \$ has been calculated for the installation of nr. 2 rotors.

- The modernisation of ship propulsion is also linked to the lack of the possibility to transport and deliver commercial materials and, consequently, to the lost earnings. In fact, a 30 k\$/day parameter has been considered as costs related to the stop of the ship for the refitting;
- Another factor that has a positive result from the use of FRs is the shortening of the usage periods of endothermic engines and the consequent time expansion of the maintenance plans associated with them, and the consequent shifting of their deadlines forward over time. For this aspect, 100 k\$/year as savings deriving from the expansion of the mean time between engine maintenance interventions;
- A direct consequence of the lower use of the engines is the necessity to maintain the rotors regularly. With regard to this, a parameter of 50 k\$/year as costs for the maintenance of the rotors has been considered. Indeed, the power absorbed by rotors while working has been calculated through the formula suggested by Pearson in his work as follows [22]:

$$P_{cyl} = \frac{1}{2} \cdot C_{M\_cyl} \cdot \rho_{air} \cdot \omega_{cyl}{}^{3} \cdot R_{cyl}{}^{4} \cdot L_{cyl} \qquad (14)$$

where $C_M$ is, together with $C_{Lift}$ and $C_{Drag}$, one of the data measured during the wind tunnel campaign [23].

Standing to the recent studies about gas emission reduction systems available on the market [41] aiming to meet the Tier III restrictions provided by MARPOL Annex IV, a rate of 0.4 has been considered between kWh and kg of $CO_2$.

This is why, considering all the parameters described above, it is possible to create a forecast based on the number of navigations made on the considered route as well as on the annual consumption and the relative earnings and to verify the times linked to the return on investment regarding the work carried out for the ship undergoing the refitting.

As visible in Figure 15, the earnings deriving from the saved fuel represent the majority of the savings as follows: this is the reason why shipping mobility through green energy has the potential to become significant.
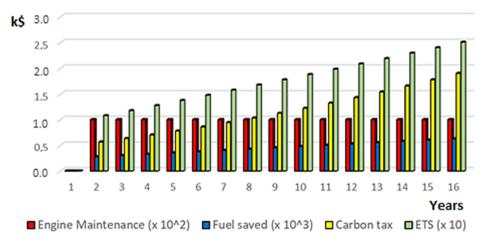


**Figure 15.** Savings estimation.

As a matter of fact, the created code can provide shipowners with the following very important decision factor: whether the installation of the rotors on a ship, which has already been in line for several years, is cost-effective before the performance decay of its other equipment or not, and therefore it is better to focus on other solutions of sustainable mobility.

To give a more heterogeneous evaluation of the return on investment related to the usage of FRs aboard cargo ships, several simulations have been conducted by matching different tracks with different speed range rotor dimensions, permuting the data available in Table 5. The arrangement of the rotors is the only parameter kept unaltered (15D in a longitudinal manner).
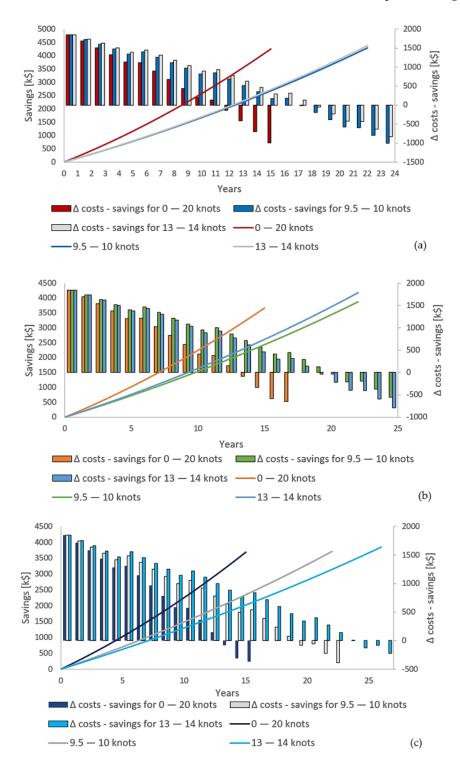
**Table 5.** Simulations executed.

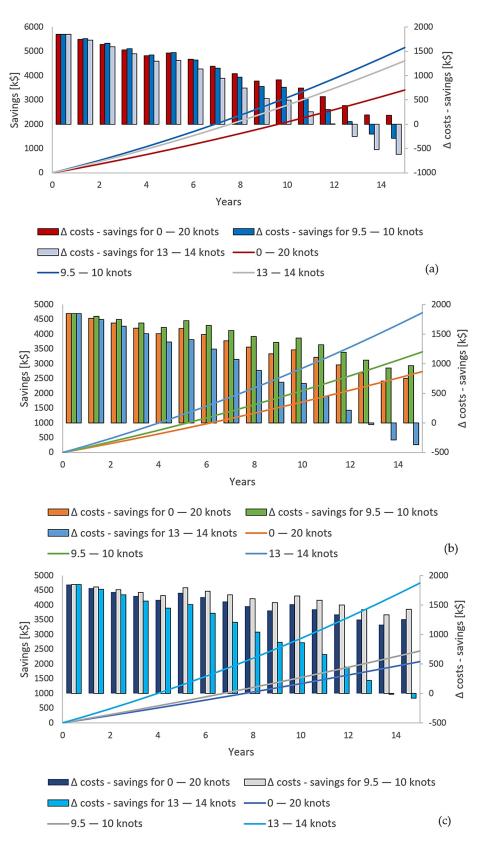| Routes | Distances |
|---|---|
| Barcelona (ESP)–Alexandria (EGP) | 1615 Nautical Miles |
| Tokyo (JAP)–Sidney (AUS) | 4629 Nautical Miles |
| Singapore–San Francisco (USA) | 7435 Nautical Miles |
| New York (USA)–Lagos (NGA) | 5010 Nautical Miles |
| **Rotors Diameter** | **Aspect Ratio** |
| 5 m | 6 |
| 3 m | 6 |
| 3 m | 8 |
| **Velocity Range** | From 0 to 20 knots |
| | From 9 to 10 knots |
| | From 13 to 14 knots |

## 5. Results

These results have been obtained by conducting a 6DOF analysis and investigating all the different values of SR available from the wind tunnel test data.
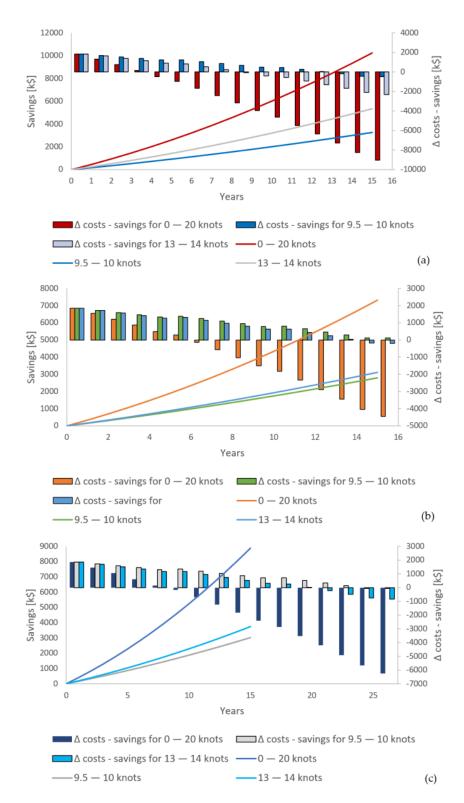
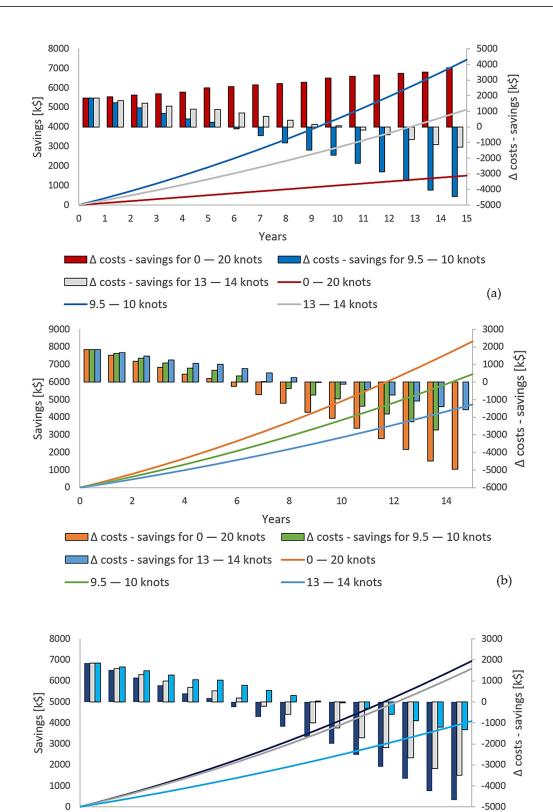These simulations have shown relevant data, which are depicted in Figures 16–19.



**Figure 16.** 6DOF simulation for a route from Barcelona to Alexandria in different rotor configurations: (**a**) D = 5 m and AR = 6; (**b**) D = 3 m and AR = 8; (**c**) D = 3 m and AR = 6.

**Figure 17.** 6DOF simulation for a route from Tokyo to Sidney in different rotor configurations: (**a**) D = 5 m and AR = 6; (**b**) D = 3 m and AR = 8; (**c**) D = 3 m and AR = 6.

**Figure 18.** 6DOF simulation for a route from Singapore to San Francisco in different rotor configurations: (**a**) D = 5 m and AR = 6; (**b**) D = 3 m and AR = 8; (**c**) D = 3 m and AR = 6.

**Figure 19.** 6DOF simulation for a route from New York to Lagos in different rotor configurations: (**a**) D = 5 m and AR = 6; (**b**) D = 3 m and AR = 8; (**c**) D = 3 m and AR = 6.

In these graphs, the bars represent the difference between costs and savings deriving from the constant usage of the rotors during navigations, while the lines highlight the savings with reference to the left *y*-axis. Each chart shows the same data for each year of work and for each one of the routes enlisted in Table 5, but with different rotor dimensions.

The results highlight the following considerations:

- If ships are free to move in the 0–20 knots range of speed, the difference between earnings and costs decreases more rapidly when compared to ships with a stricter range of speed. This behaviour is particularly evident in the case study of the ship travelling from New York to Lagos;
- In the tracks crossing an ocean, the ship encounters more constant and deep winds, if compared to the Mediterranean Sea;
- The Atlantic Ocean is windier than the Western Pacific one, so dimensions proportionally influence the number of years necessary for the return on investment. This result can find the same evidence in the paper by Traut et al. [42], where a simulation of a ship sailing the Atlantic Ocean is analysed;
- For the crossing of the Pacific Ocean, a ship spacing within a wider speed range (0–20 knots) retrieves the initial investments in almost half the time if compared to the same ship when obliged within a thinner speed range, independently from the dimensions of the rotors;
- For ships operating in calm and closed seas such as the Mediterranean one and obliged to have a mean speed of 14 knots, rotors having D = 3 m and AR = 8 are eligible, while if no restrictions on the speed are imposed, the simulation using the wider speed range suggests the 5m x 6 configuration as the best one;
- In the Tokyo-to-Sidney route, the 13–14 knots speed range guarantees the shortest period for the return on investment.

## 6. Conclusions

This work shows how FRs are a valid solution in terms of $CO_2$ emission reduction in the environment, and they represent an always more interesting field for shipping companies and military fleets [43], considering the almost free-of-charge use of the wind power and the consequent fuel savings.

The created power prediction program was tested only with the weather data of 4 July 2022. Given the heterogeneity of weather and sea conditions a ship can encounter during a voyage, the results could be affected by a consistent percentage of correction if specific picks of wind and wave values are recorded and analysed. Nevertheless, this PPP aims to optimise the effectiveness of the rotating towers as an alternative propulsion while preserving the ship 6DOF stability and manoeuvrability during the route by solving the force and moment balance equations.

The code presented in this paper is a valid tool, alternative to the NAPA Voyage Optimization software, to provide users with a techno-economic analysis for the calculation of the best route and simulating costs and savings related to the usage of Flettner rotors.

As eligible in Figures 16–19, the solution offered by these towers to the economic problem linked to the shipping environment binomial is certainly interesting, especially if we consider a return on the initial investment and an increase in profit margins compared to the use of endothermic combustion engines starting from approx. 10 to 12 years after installing the rotors.

Important conclusions are as follows:

- The relevance of the geographical area where the ships sail in, while using wind propulsion. In fact, significant results have been obtained in terms of return on investment for a ship sailing in oceans since they offer better wind conditions to be exploited for the work of the rotors if compared to the Mediterranean Sea;
- For the Mediterranean route (Barcelona to Alexandria), the payback period is the same when rotors are considered in all three configurations if the speed range is kept wider (0–20 knots) or low (9–11 knots). This can be ascribed to the less intensive winds

characterising the closer seas and the difference in thrust, which the FRs having D = 3 and AR = 6 would provide to maintain the shipping speed between 13 and 14 knots;
- For the route from New York to Lagos as well as for the one from Singapore to San Francisco, the wider range of 0–20 knots of available speed range returns for a better optimisation of the FRs, due to the wider spectrum of wind and waves, which can be encountered;
- Calculations regarding the Singapore-to-San Francisco, as well as the New York-to-Lagos routes, shows that the smaller configuration of FRs does not fully exploit the potential of wind-assisted propulsion, if compared to the other configurations and especially when the 13–14 knots speed is required;
- Particular mention is deserved by the simulation regarding the route from Tokyo to Sydney since the weather data were especially favourable and allowed the best usage of FRs in the highest speed range available, guaranteeing contemporarily the shortest travelling time (it is interesting to notice that for the configuration with smaller rotors, the number of years necessary to cover the difference between savings and costs widely exceeds 18 years).

Furthermore, the calculations have led to the following additional conclusions: the further the arrival point, the stricter the time in years necessary to cover the initial investment and the bigger the rotor diameter, the more effective the rotor contribution to the ship propulsion.

In conclusion, the potential of Flettner rotors as a marine propulsion system highlight that drag and lift can provide a positive contribution to the thrust for a wide range of wind angles, reducing the ship resistance up to 25%. Surely further studies should be conducted to validate the assumptions and the results related to the fuel-saving benefits an FR installation may imply.

Considering the evident benefits highlighted in the present study about Flettner rotors and considering the actual focus of the International Classification Societies and Flag Authorities on $CO_2$ emission reductions, it might be interesting to check the earnings and transport volumes of the next 5, 10, and 20 years of companies deciding to embrace this wind propulsion solution today and to compare them with those of the companies adopting other alternative energy solutions or new exhaust gas treatment systems for endothermic engines.

## References

1. European Commission. *2020 Annual Report on CO₂ Emissions from Maritime Transport*; European Commission: Brussel, Belgium, 2021.
2. Zhang, P.; Lozano, J.; Wang, Y. Using Flettner Rotors and Parafoil as alternative propulsion systems for bulk carriers. *J. Clean. Prod.* **2021**, *317*, 128418. [CrossRef]
3. Ammar, N.R.; Seddiek, I.S. Wind assisted propulsion system onboard ships: Case study Flettner rotors. *Ships Offshore Struct.* **2021**, *17*, 1616–1627. [CrossRef]

4.   Schönborn, A. Combination of propulsive thrust and rotational power for ships from a cyclic pitch Darrieus rotor sail. *Sustain. Energy Technol. Assessments* **2022**, *52*, 102008. [CrossRef]

5.   Kramer, J.; Steen, S.; Savio, L. Drift forces–Wingsails vs Flettner rotors. High performance marine vehicles. In Proceedings of the High-Performance Marine Vehicles, Cortona, Italy, 3–8 July 2016.

6.   Traut, M.; Gilbert, P.; Walsh, C.; Bows, A.; Filippone, A.; Stansby, P.; Wood, R. Propulsive power contribution of a kite and a Flettner rotor on selected shipping routes. *Appl. Energy* **2014**, *113*, 362–372. [CrossRef]

7.   Al-Enazi, A.; Okonkwo, E.C.; Bicer, Y.; Al-Ansari, T. A review of cleaner alternative fuels for maritime transportation. *Energy Rep.* **2021**, *7*, 1962–1985. [CrossRef]

8.   Povarov, V.G.; Efimov, I.; Smyshlyaeva, K.I.; Rudko, V.A. Application of the UNIFAC Model for the Low-Sulfur Residue Marine Fuel Asphaltenes Solubility Calculation. *J. Mar. Sci. Eng.* **2022**, *10*, 1017. [CrossRef]

9.   Lu, R.; Ringsberg, J. Ship energy performance study of three wind-assisted ship propulsion technologies including a para-metric study of the Flettner rotor technology. *Ships Offshore Struct.* **2020**, *16*, 249–258. [CrossRef]

10.   Sandurawan, D.; Kodikara, N.; Keppitiyagama, C.; Rosa, R. A Six Degrees of Freedom Ship Simulation System for Maritime Education. *Int. J. Adv. ICT Emerg. Reg. (ICTer)* **2011**, *3*, 34. [CrossRef]

11.   Taimuri, G.; Matusiak, J.; Mikkola, T.; Kujala, P.; Hirdaris, S. A 6-DoF maneuvering model for the rapid estimation of hydro-dynamic actions in deep and shallow waters. *Ocean. Eng.* **2020**, *218*, 108103. [CrossRef]

12.   Fischer, S.; Gluch, M.; Benedict, K.; Klaes, S.; Krüger, C.; Baldauf, M. Application of Fast Time Manoeuvring Simulation for Training of Challenging Situations in Voyage Planning at Arrival & Departure and for Collision Avoidance. In Proceedings of the 20th International Navigation Simulator Lecturers Conference, Auckland, New Zealand, 10–13 September 2018.

13.   Sprenger, F.; Maron, A.; Delefortrie, G.; Van Zwijnsvoorde, T.; Cura-Hochbaum, A.; Lengwinat, A.; Papanikolaou, A. Experimental studies on seakeeping and maneuverability of ships in adverse weather conditions. *J. Ship Res.* **2017**, *10*, 131–152. [CrossRef]

14.   Tillig, F.; Ringsberg, J.W. A 4 DOF simulation model developed for fuel consumption prediction of ships at sea. *Ships Offshore Struct.* **2018**, *14*, 112–120. [CrossRef]

15.   Savonius, S.J. *The Wing Rotor in Theory and Practice*; LAP LAMBERT Academic Publishing: London, UK, 1925.

16.   Flettner, A. The Flettner rotor-ship. *Sci. Act.* **1971**, *6*, 10–14.

17.   Prandtl, L. The Magnus effect and wind-powered ships. *Naturwissenschaften* **1925**, *13*, 1787–1806.

18.   Thom, A. *Effect of Discs on the Air Forces on a Rotating Cylinder*; AERADE: Inner Hebrides, UK, 1934.

19.   Craft, T.; Iacovides, H.; Launder, B. Dynamic performance of Flettner Rotors with and without Thom discs. In *Seventh International Symposium on Turbulence and Shear Flow Phenomena*; Begel House Inc.: Danbury, CO, USA, 2011.

20.   De Marco, A.; Mancini, S.; Pensa, C.; Calise, G.; De Luca, F. Flettner Rotor Concept for Marine Applications: A Systematic Study. *Int. J. Rotating Mach.* **2016**, *2016*, 1–12. [CrossRef]

21.   Zhang, W.; Bensow, R. Numerical simulation of high-Reynolds number flow around Flettner rotors. In Proceedings of the 14th Numerical Towing Tank Symposium, Dorset UK, 22–24 October 2011.

22.   Pearson, D. The Use Of Flettner Rotors In Efficient Ship Design. In Proceedings of the Influence of EEDI on Ship Design Conference, London UK, 24–25 December 2014.

23.   Bordogna, G. *Aerodynamics of Wind-Assisted Ships*; Delft University of Technology: Delft, The Netherlands, 2020.

24.   Enercon GmbH. Enercon E-Ship 1-A Wind-Hybrid Commercial Cargo Ship. In Proceedings of the Conference on Ship Efficiency, Hamburg, Germany, 23–24 September 2013.

25.   Hotrop, J.; Mennen, G.G.J. *An Approximate Power Prediction Method*; Delft TU: Delft, The Netherlands, 1982.

26.   Hotrop, J.; Mennen, G.G.J. *A Statistical Power Prediction Method*; Delft TU: Delft, The Netherlands, 1978.

27.   Liu, S.; Papanikolau, A. Fast approach to the estimation of the added resistance of ships in head-waves. *Ocean Engineering* **2016**, *112*, 211–225. [CrossRef]

28.   Berendschot, R. *Flettner Rotor Vessel Design Optimization*; Delft TU: Delft, The Netherlands, 2019.

29.   Nomoto, K.; Taguchi, T.; Keinosuke, H.; Susumu, H. On the steering qualities of ships. *Int. Shipbuild. Prog.* **1957**, *4*, 354–370. [CrossRef]

30.   Clarke, D.; Gedling, P.; Hine, G. *The Application of Maneuvering Criteria in Hull Design Using Linear Theory*; Delft University of Technology: Delft, The Netherlands, 1982.

31.   Dijkstra, E.W. A note on two problems in connexion with graphs. *Numer. Math.* **1959**, *1*, 269–271. [CrossRef]

32.   Silveira, P.; Teixeira, A.; Soares, C.G. AIS Based Shipping Routes Using the Dijkstra Algorithm. *TransNav, Int. J. Mar. Navig. Saf. Sea Transp.* **2019**, *13*, 565–571. [CrossRef]

33.   Musolino, G.; Gattuso, D. Modelli di costo del trasporto marittimo in container e di interscambio modale. In *Metodi e Tecnologie dell'Ingegneria dei Trasporti. Seminario 2000*; Franco Angeli: Reggio Calabria, Italy, 2002.

34.   Norway Government. *White Paper Climate Action Plan 2021–2030*; Norway Government: Oslo, Norway, 2020.

35.   EMSA. *European Maritime Transport Environmental Report*; EMSA: Brussel, Belgium, 2021.

36.   Tsiropoulos, I.; Nijs, W.; Tarvydas, D.; Castello, P.R. *Towards Net-Zero Emissions in the EU Energy System by 2050*; Publications Office of the European Union: Brussel, Belgium, 2020.

37.   World Bank. *State and Trends of Carbon Pricing 2021*; World Bank: Washington, DC, USA, 2021. [CrossRef]

38. Badalamenti, C.; Prince, S. Effects of Endplates on a Rotating Cylinder in Crossflow. In Proceedings of the 26th AIAA Applied Aerodynamics Conference, Honolulu, HI, USA, 3–6 July 2008. [CrossRef]

39. Apostolidis, A.; Merikas, A.; Merika, A. The Modelling of Maintenance Cost: The Case of Container-Ships in Dry-Dock. *J. Comput. Optim. Econ. Financ.* **2013**, *5*, 27.

40. Apostolidis, A.; Kokarakis, J.; Merikas, A. Modeling the Dry-Docking Cost—The Case of Tankers. *J. Ship Prod. Des.* **2012**, *28*, 134–143. [CrossRef]

41. Lindstad, H.; Eskeland, G.S.; Psaraftis, H.; Sandaas, I.; Strømman, A.H. Maritime shipping and emissions: A three-layered, damage-based approach. *Ocean Eng.* **2015**, *110*, 94–101. [CrossRef]

42. Traut, M.; Bows, A.; Gilbert, P.; Mander, S.; Stansby, P.; Walsh, C.; Wood, R. Low C for the high seas: Flettner rotor power con-tribution on a route Brazil to UK. In Proceedings of the Low Carbon Shipping conference, Newcastle, UK, 8–12 June 2012.

43. Naval Sea Systems Command Department of the Navy. *Magnus Effect—An Overview of Its Past and Future Practical Applications*; United Nations: New York, NY, USA, 1986.